SCIENCE CHINA
Life Sciences

Tsinghua Special Issue
• RESEARCH PAPER •

January 2014 Vol.57 No.1: 59–68
doi: 10.1007/s11427-013-4588-8

Atg5 regulates late endosome and lysosome biogenesis

PENG JunYa[1], ZHANG Ran[1], CUI YiTong[1], LIU HaoDong[1], ZHAO XiaoXin[1], HUANG Lei[2], HU MingXu[1], YUAN XiaoXi[4], MA BenYu[4], MA XiaoWei[5], TAKASHI Ueno[6], MASAAKI Komatsu[7], LIANG XingJie[3] & YU Li[1*]

[1]*State Key Laboratory of Biomembrane and Membrane Biotechnology, Tsinghua University-Peking University Joint Center for Life Sciences, School of Life Science, Tsinghua University, Beijing 100084, China;*
[2]*Cell Biology Core Facility, School of Life Science, Tsinghua University, Beijing 100084, China;*
[3]*Department of Mathematical Sciences, Tsinghua University, Beijing 100084, China;*
[4]*Tsinghua University-Peking University Joint Center for Life Sciences, School of Life Science, Tsinghua University, Beijing 100084, China;*
[5]*Laboratory of Nanomedicine and Nanosafety, Division of Nanomedicine and Nanobiology, National Center for Nanoscience and Technology, China, and CAS Key Laboratory for Biomedical Effects of Nanomaterials and Nanosafety, Chinese Academy of Sciences, Beijing 100190, China;*
[6]*Department of Biochemistry, Juntendo University School of Medicine, Bunkyo-ku, Tokyo 1138421, Japan;*
[7]*Protein Metabolism Project, Tokyo Metropolitan Institute Medical Science, Tokyo 1568506, Japan*

Received October 16, 2013; accepted November 22, 2013; published online December 23, 2013

Autophagy is an evolutionarily conserved lysosome-based degradation process. Atg5 plays a very important role in autophagosome formation. Here we show that Atg5 is required for biogenesis of late endosomes and lysosomes in an autophagy-independent manner. In *Atg5*$^{-/-}$ cells, but not in other essential autophagy genes defecting cells, recycling and retrieval of late endosomal components from hybrid organelles are impaired, causing persistent hybrid organelles and defective formation of late endosomes and lysosomes. Defective retrieval of late endosomal components from hybrid organelles resulting from impaired recruitment of a component of V1-ATPase to acidic organelles blocks the pH-dependent retrieval of late endosomal components from hybrid organelles. Lowering the intracellular pH restores late endosome/lysosome biogenesis in *Atg5*$^{-/-}$ cells. Our data demonstrate an unexpected role of Atg5 and shed new light on late endosome and lysosome biogenesis.

endosome/lysosome biogenesis, atg5, autophagy

Citation: Peng JY, Zhang R, Cui YT, Liu HD, Zhao XX, Huang L, Hu MX, Yuan XX, Ma BY, Ma XW, Takashi U, Masaaki K, Liang XJ, Yu L. Atg5 regulates late endosome and lysosome biogenesis. Sci China Life Sci, 2014, 57: 59−68, doi: 10.1007/s11427-013-4588-8

The biogenesis of lysosomes is a relatively poorly understood subject [1–6]. Various competing but not mutually exclusive models of lysosome biogenesis have been proposed, with the "kiss and run" and "hybrid" models the current main contenders. In the "kiss and run" model [7], the contents of late endosomes are delivered to lysosomes through transient fusion events, while in the "hybrid" model, late endosomes and lysosomes fuse completely to form hybrid organelles, and lysosomes are then formed through selective retrieval of late endosomal components from the hybrid organelles [8].

Autophagy is a lysosome-based degradation process that is conserved in all eukaryotes [9,10]. During autophagy, intracellular contents including cytosol and organelles are engulfed by double-membrane vesicles named autophagosomes. Autophagosomes then fuse with lysosome to form a hybrid organelle named autolysosome, within which engulfed intracellular contents are degraded [11]. Autophagy

*Corresponding author (email: liyulab@mail.tsinghua.edu.cn)

plays many important physiological roles in cell survival, pathogen clearance, lipid metabolism and protein aggregate removal [10,12]. Abnormal autophagy is linked to various diseases including neurodegenerative diseases, cancer, and autoimmunity [13,14]. Atg5 is one of these "autophagy essential genes" which is required for autophagosome formation. The majority of Atg5 are conjugated to Atg12 at Lys149 through an isopeptidebond [15]. The formation of the Atg5-Atg12 conjugates is constitutive and occurs soon after the proteins are synthesized [16]. Atg5-Atg12 has E3 like activity which can facilitate the Atg8/LC3-PE conjugation.

In this manuscript, we have shown that Atg5 is essential for the biogenesis of late endosomes and lysosomes. In *Atg5*$^{-/-}$ cells, the recycling and retrieval of late endosomal components from hybrid organelles are impaired, which causes formation of permanent hybrid organelles, thus resulting in defective late endosome/lysosome biogenesis. We found that the defective retrieval of late endosomal components from hybrid organelles is caused by impaired recruitment of a subunit of V1-ATPase to acidic organelles, resulting in the elevation of pH in acidic organelles. This subsequently blocks the retrieval of late endosomal components from hybrid organelles by the retromer, which is dependent on low pH. Lowering intracellular pH by maintaining cells in low pH buffer restores late endosome/lysosome biogenesis in *Atg5*$^{-/-}$ cells. Thus, Atg5 regulates late endosome and lysosome biogenesis through regulating lysosomal pH.

1 Materials and methods

1.1 Antibodies and reagents

The following antibodies were used in this study: anti-Atg5 (#8540s; Cell Signaling, Boston, USA), anti-Atg7 (#2631S; Cell Signaling), anti-LAMP1 (L1418; Sigma, St. Louis, USA), anti-LAMP2 (L0668; Sigma), anti-Actin (A2066; Sigma), and anti-Vatpase D (sc-166218; Santa Cruz, Dallas, USA). The reagents used in this study are as follows: leupeptinhemisulfate salt (L2884; Sigma), Lysotracker-red (23073w; Invitrogen, New York, USA), Rhodamine B isothiocyanate-Dextran (MW70000, R9379; Sigma), Fluorescein isothiocyanate Dextran (MW70000, FD70S; Sigma). Lysosome isolation kit (LYSISO1; Sigma), BCA Protein Assay Reagent (Thermo Scientific, Waltham, USA), 13 nm gold nanoparticles were kindly provided by Dr. Liang XingJie (National Center for Nanoscience and Technology, China). Acidification of media and pH-induction assays were performed as previously described.

1.2 Cell culture and transfection

MEF cells (wild type, *Atg5*$^{-/-}$) were obtained from Dr. Noboru Mizushima. NRK cells were from the American Type Culture Collection. Cells were cultured in DMEM (Hyclone, Waltham, USA) medium supplemented with 10% FBS (5% CO_2), glutamax and penicillin-streptomycin. Cells were transfected with 200 pmol siRNA or no more than 5 μg DNA via Amaxanucleofector^{TM} II using a MEF2 kit and program T-020 (for MEF cells), or solution T and program X-001 (for NRK cells). Cells were then cultured in growth medium for further analysis. For four rounds of transfection, cells were transfected with 200 pmol siRNA, and 72 h after transfection, cells were transfected again with 200 pmol siRNA; this procedure was then repeated.

1.3 Lentiviral infection

Transfection was performed with ViraPower™ Promoterless Lentiviral Gateway® Kits (Invitrogen). Plasmid construction and lentivirus transfection were performed according to the manufacturer's manual.

1.4 Constructs

LAMP1 constructs with CFP, GFP, RFP, CI-MPR-GFP and EEA-YFP were provided by Dr. J. Lippincott-Schwartz, NICHD, NIH. siRNAs and shRNA were synthesized by GenePharma (Shanghai): atg5, GGCATTATCCAATTGGCCTACTGTT; atg7, CCTGTTCATCCAAAGTTCTTGATCA; V-ATPase D, CCAAAGCAGTGGAACTACTGGTGGA; atg12, GGTTAGAAAGGAGACTGGAATTCTA.

1.5 Live cell imaging

Transfected cells were re-plated in Lab Tek Chambered Coverglasses (NUNC) 24 h before live cell imaging. Cells were maintained at 37°C with 5% CO_2 in a PeCon open chamber (PeCon, Erbach, Germany) system. Images were captured by Olympus FV-1000 confocal microscope and laser-based Spinning Disk confocal microscopy system.

1.6 Cell homogenization and endocytic vesicle purification

Cells were incubated with 5 nmol 13 nm gold nanoparticles in the growth medium for 4 h. The cells were then washed three times in phosphate buffer (PBS). After harvesting, cell pellets were resuspended in 1 mL homogenization buffer (0.25 mol L^{-1} sucrose, 3 mmol L^{-1} imidazole and 0.5 mmol L^{-1} EDTA, pH 7.3) and pelleted again at 1000×*g* for 10 min. The pellet was resuspended in 1 mL homogenization buffer and broken in a Dounce homogenizer until the nuclei were still intact as seen by light microscopy. After homogenization, the gold-filled fraction was pelleted together with the nuclei at 1000×*g* for 10 min. The pellet was resuspended in 2.5 mL 17% Percoll and loaded onto a 2 mL 64% sucrose

cushion in a 6 mL Beckman ultracentrifuge tube. The samples were centrifuged for 30 min at 27000×*g* in a Beckman SW55Ti rotor with fast acceleration. After this run, the nuclear fraction remained at the top whereas the gold-filled organelles were at the bottom of the sucrose cushion. The bottom pellet was resuspended in protein loading buffer.

1.7 Staining

Cells were washed with phosphate buffered saline (PBS) and fixed in 4% paraformaldehyde (room temperature) or methanol (–20°C) for 10 min. Cells were then blocked with 10% FBS in PBS for 20 min, stained with the first antibody in blocking buffer with 0.1% (w/v) saponin for 1 h, and washed with PBS three times. Cells were then stained with secondary antibody (Invitrogen) in blocking buffer with 0.1% (w/v) saponin for 1 h and washed with PBS three times. The cells were mounted with Fluoromount-G (#0100-01; SouthernBiotech, Birmingham, USA).

1.8 Electron microscopy

Cells were fixed in 3% glutaraldehyde in 0.1 mol L^{-1} MOPS buffer (pH 7.0) for 8 h at room temperature, then 3% glutaraldehyde/1% paraformaldehyde in 0.1 mol L^{-1} MOPS buffer (pH 7.0) for 16 h at 4°C. They were then post-fixed in 1% osmium tetroxide for 1 h, and embedded in Spurr's resin, sectioned, doubly stained with uranyl acetate and lead citrate, and analyzed using a Hitachi H-7650 transmission electron microscope.

2 Results

2.1 Late endosome and lysosome biogenesis is impaired in *Atg5*$^{-/-}$ mouse embryonic fibroblast (MEF) cells

We observed an abnormality in Lamp1-positive organelles (LPOs) in *Atg5*$^{-/-}$ MEF cells maintained in nutrient-rich medium; in these cells, LPOs are reduced in number and increased in size (Figure 1A and B). To make sure that the LPO abnormality is not a developmental artifact, we transfected Atg5 back into *Atg5*$^{-/-}$ MEF cells respectively, and found that the abnormal LPO phenotype was rescued (Figure 1C–E). We also knocked down the expression level of Atg5 in normal rat kidney (NRK) cells, and observed a similar LPO phenotype as in *Atg5*$^{-/-}$ MEF cells (Figure 1F–H).

2.2 Free Atg5 regulates late endosome/lysosome biogenesis in an autophagy independent manner

Next, we test whether the role of Atg5 in regulating LPOs is autophagy-dependent. For this purpose, we established NRK cell lines in which autophagy essential genes, including Atg7, Atg9, and Atg12 were stably knocked down (Figure 2). We found there were no significant differences of LPOs' numbers and size between NS and Atg7, Atg9 and Atg12 knockdown cells. These data indicates that Atg5 regulates late endosome/lysosome biogenesis in an autophagy independent manner. The fact that knocking down Atg12 has no effect on LPOs suggests that it is the free Atg5 that regulates LPO biogenesis.

2.3 Late endososme/lysosome biogenesis is arrested at the hybrid organelle stage

LPOs are composed of two different organelles, lysosomes and late endosomes, which can be distinguished by morphology, molecular markers and accumulation of endocytic tracers [7]. Morphologically, lysosomes are heterogeneous, often spherical, and appear electron-dense by transmission electron microscopy (TEM); in contrast, late endosomes are often tubular in shape, and contain close-packed vesicles. Molecularly, late endosomes are positive for M6PR while lysosomes are not [17]. Finally, because lysosomes are the terminal organelles in the endocytic pathway while late endosomes are the intermediate organelles, tracers such as dextran and nano-gold particles pass through late endosomes soon after uptakes and eventually reach lysosomes, where they stay for a long period of time [7]; thus, lysosomes can be selectively labeled by treating cells with a pulse of tracer followed by a prolonged chase period [7]. Based on these criteria, we classify spherical, dextran/nano-gold particle-positive, cation-independent mannose-6-phosphate receptor (CI-M6PR)-negative organelles with electron-dense cores as lysosomes; and tubular, CI-M6PR-positive, dextran/nano-gold particle-negative organelles with packed vesicles in the lumen as late endosomes.

Labeling CI-M6PR-expressing wild type MEF cells with dextran for 4 h followed by a 20 h chase period revealed the presence of late endosomes and lysosomes. We also observed M6PR-positive, dextran-positive organelles (Figure 3A). The presence of markers for both late endosomes and lysosomes indicates that these structures are hybrid organelles. To confirm this, we labeled cells by pulse-chasing with nano-gold particles using a similar time-course as for dextran, and analyzed the labeled cells by TEM. As well as observing typical lysosomes, we found that a fraction of organelles containing both packed vesicles and dense cores are labeled by nano-gold particles, and are thus hybrid organelles (Figure 3B).

We observed abundant tubular LPOs in wild type MEFs; however, these tubular LPOs are largely absent in *Atg5*$^{-/-}$ MEF cells, suggesting that there are no late endosomes in these cells (Figure 3C and D). Most LPOs in *Atg5*$^{-/-}$ cells are both M6PR-positive and dextran-positive, indicating that they are hybrid organelles (Figure 3E and F). TEM analysis revealed that almost all lysosome/late endosome-like vesicles in *Atg5*$^{-/-}$ cells contain packed vesicles and dense cores (Figure 3G and H), and TEM analysis of nano-gold particle-labeled cells revealed that these are in-

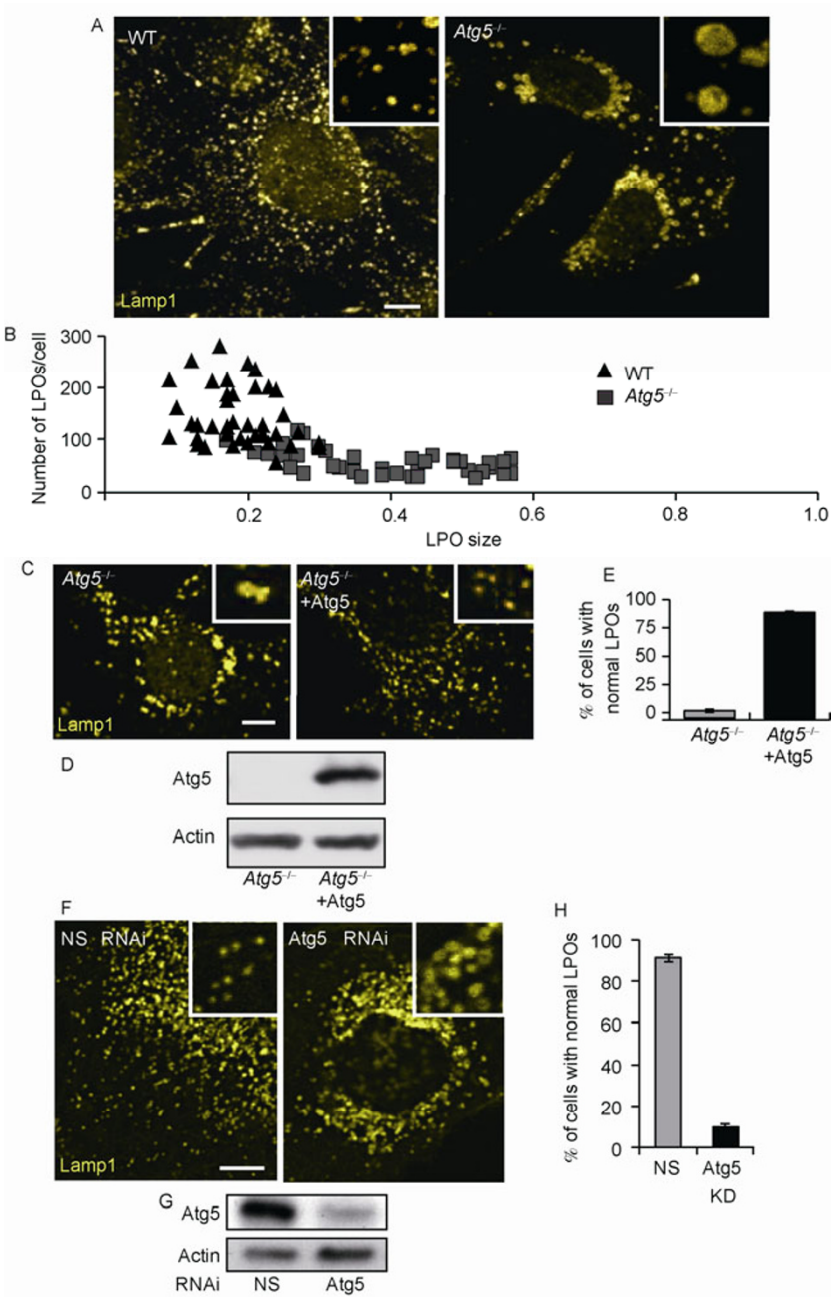

Figure 1 Atg5 regulates the number and morphology of late endosomes/lysosomes. A, Wild type, *Atg5*$^{-/-}$ MEF cells were stained with antibody against Lamp1 and observed by confocal microscopy. Scale bar, 5 μm. Inserts show enlarged regions of interest. B, Cells from (A) were quantified for the number and size of Lamp1-positive organelles (LPOs) in a blind fashion. Each symbol on the plot represents an individual cell. C, *Atg5*$^{-/-}$ cells were transfected with Atg5 respectively by lentivirus-mediated transfection. Cells were stained with antibody against Lamp1 and observed by confocal microscopy. Scale bar, 5 μm. Inserts show enlarged regions of interest. D, Cells from (C) were analyzed for the expression level of Atg5 by Western blot. E, Cells from (C) were assessed and quantified for normal LPOs in a blind fashion. One hundred cells were counted. Error bars indicate the standard deviation. F, NRK cells were transfected with nonspecific (NS)-, Atg5-RNAi for four rounds. Cells were stained with antibody against Lamp1 and observed by confocal microscopy. Scale bar, 5 μm. Inserts show enlarged regions of interest. G, Cells from (F) were analyzed for the expression level of Atg5 by Western blot. H, Cells from (F) were assessed and quantified for normal LPOs in a blind fashion. One hundred cells were counted. Error bars indicate the standard deviation.

deed hybrid organelles as they are all positive for nano-gold particles (Figure 3I and J). Taken together, we conclude that late endosome/lysosome formation is impaired in Atg5-defective cells and late endosome/lysosome biogenesis is arrested at the hybrid organelle stage.

2.4 Tubulation and tubulation mediated fission of late endosome are impaired in *Atg5*$^{-/-}$ MEFs

It has been proposed that lysosomes can be formed by retrieving late endosome components from hybrid organelles

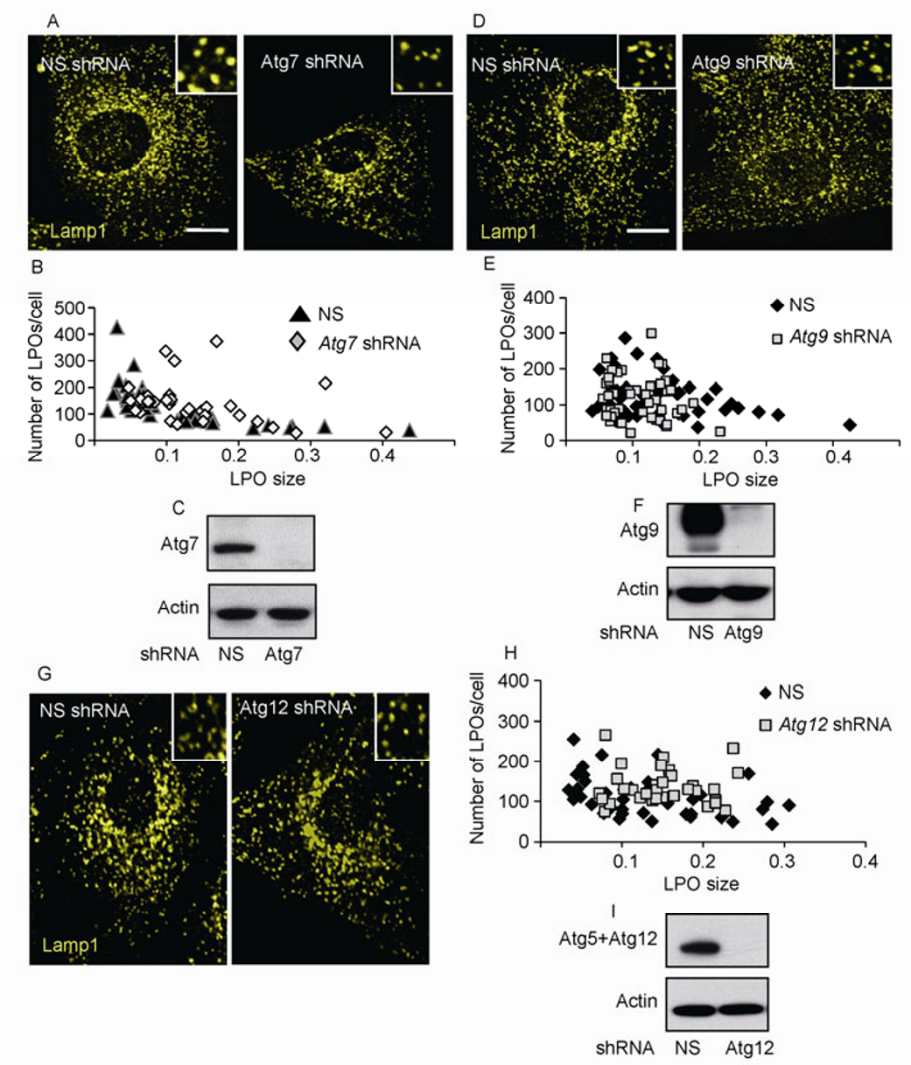

Figure 2 Regulation of LPOs by Atg5 is autophagy independent. A, NRK cells stably express nonspecific (NS) and Atg7 shRNA. Cells were stained with antibody against Lamp1 and observed by confocal microscopy. Scale bar, 5 μm. Inserts show enlarged regions of interest. B, Cells from (A) were quantified for the number and size of Lamp1-positive organelles (LPOs) in a blind fashion. Each symbol on the plot represents an individual cell. C, Cells from (A) were analyzed for the expression level of Atg7 by Western blot. D, NRK cells stably express nonspecific (NS) and Atg9 shRNA. Cells were stained with antibody against Lamp1 and observed by confocal microscopy. Scale bar, 5 μm. Inserts show enlarged regions of interest. E, Cells from (D) were quantified for the number and size of Lamp1-positive organelles (LPOs) in a blind fashion. Each symbol on the plot represents an individual cell. F, Cells from (D) were analyzed for the expression level of Atg9 by Western blot. G, NRK cells stably express nonspecific (NS) and Atg12 shRNA. Cells were stained with antibody against Lamp1 and observed by confocal microscopy. Scale bar, 5 μm. Inserts show enlarged regions of interest. H, Cells from (G) were quantified for the number and size of Lamp1-positive organelles (LPOs) in a blind fashion. Each symbol on the plot represents an individual cell. I, Cells from (G) were analyzed for the expression level of Atg12 by Western blot.

[8]. We indeed observed that hybrid organelles in wild type cells are undergoing constant tubulation, and repeated tubulation can lead to fission of small Lamp1-positive vesicles from hybrid organelles. In contrast, in *Atg5*$^{-/-}$ cells, the tubulation and fission process are impaired (Figure 4A). In wild type MEFs, there are small, round LPOs which are both M6PR- and dextran-negative (Figure 3A). Since these small LPOs are dramatically reduced in Atg5$^{-/-}$ cells, we hypothesized that they may be formed from tubulation and fission of hybrid organelles. To test this hypothesis, we transfected cells with photo-active GFP-tagged Lamp1 (Lamp1-PA-GFP), and 24 h after transfection, we visualized the LPOs by activating them with a 405 nm laser. We found that 2.5 h after photo activation, the number of PA-GFP-positive LPOs increased more than 3-fold in wild type MEFs; however, in *Atg5*$^{-/-}$ MEFs, the number of PA-GFP-positive LPOs slightly decreased (Figure 4B and C). This implies that the impairment of tubulation and fission in *Atg5*$^{-/-}$ MEF cells can lead to defective formation of small Lamp1 vesicles. The fact that late endosomes are totally lacking in autophagy-null cells, together with our observation that small LPOs derived from tubulation can fuse with early endosome antigen 1 (EEA1)-labeled early endosomes (Figure S1 in Supporting Information), raises the

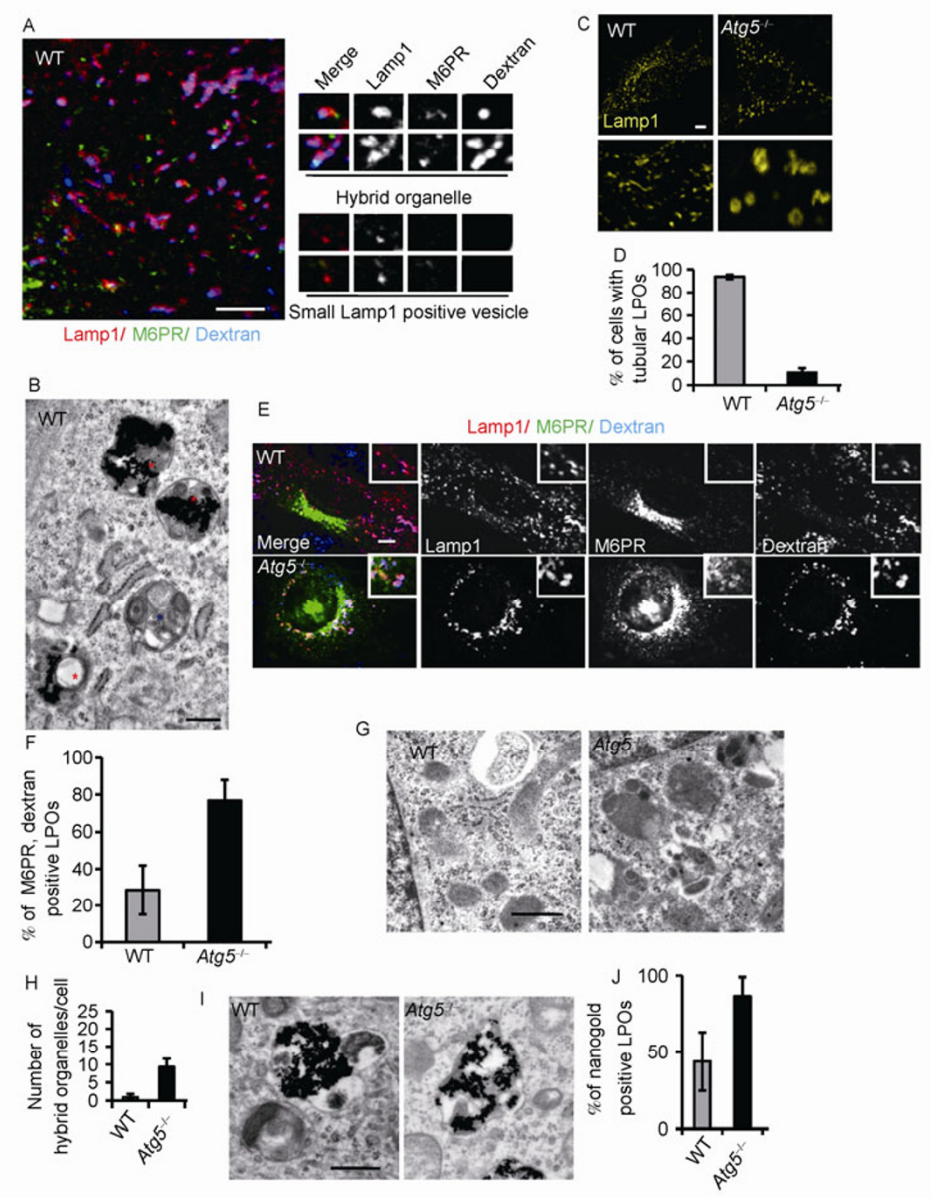

Figure 3 Defective late endosome and lysosome formation in *Atg5*$^{-/-}$ cells. A, CI-M6PR-GFP, Lamp1-CFP-expressing wild type MEF cells were labeled with Rhodamine B-labeled dextran (MW70000) for 4 h; cells were washed and grown for another 20 h before imaging. Right panel shows enlarged region of interest. Scale bar, 5 μm. B, Wild type MEF cells were labeled with nano-gold particles (13 nm) for 4 h; cells were washed and grown for another 20 h before imaging. Scale bar, 500 nm. Red star, hybrid organelle; blue star, late endosome. C, Lamp1-cherry red-expression wild type, *Atg5*$^{-/-}$ MEF cells were observed by confocal microscopy. Scale bar, 5 μm. D, Cells from (C) were assessed and quantified for presence of tubular LPOs. Fifty cells were counted. Error bars indicate the standard deviation. E, Wild type, *Atg5*$^{-/-}$ MEF cells were transfected with CI-M6PR-GFP and Lamp1-CFP; 18 h after transfection, load Rhodamine B dextran (MW 70000) for 4 h; cells were washed and grown for another 20 h before imaging. Scale bar, 5 μm. F, Cells from (E) were assessed and quantified for presence of CI-M6PR, Dextran double positive LPOs. Fifty cells were counted. Error bars indicate the standard deviation. G, Representative transmission electron micrographs of wild type, *Atg5*$^{-/-}$ MEF cells. Scale bar, 2 μm. H, Cells from (G) were assessed and quantified for the number of hybrid organelle per cell. Fifty cells were counted. Error bars indicate the standard deviation. I, Wild type, *Atg5*$^{-/-}$ MEF cells were labeled with nano-gold particles (13 nm) for 4 h; cells were washed and grown for another 20 h and analyzed by TEM. Scale bar, 500 nm. J, Cells from (I) were assessed and quantified for nano-gold particle positive LPOs. Twenty cells were counted. Error bars indicate the standard deviation.

possibility that late endosome formation requires small LPOs retrieved from hybrid organelles.

2.5 Impaired retrieval of late endosome components in *Atg5*$^{-/-}$ MEF cells

Endosome tubulation, tubular based carrier formation and retrieval of late endosome components are mediated by retromer [18]. Defective endosome tubulation in autophagy null cells implies that the retromer mediated retrieval of late endosome components is likely compromised. Retromer is composed by a membrane deformation subcomplex and a cargo selective adaptor complex. The membrane defor-

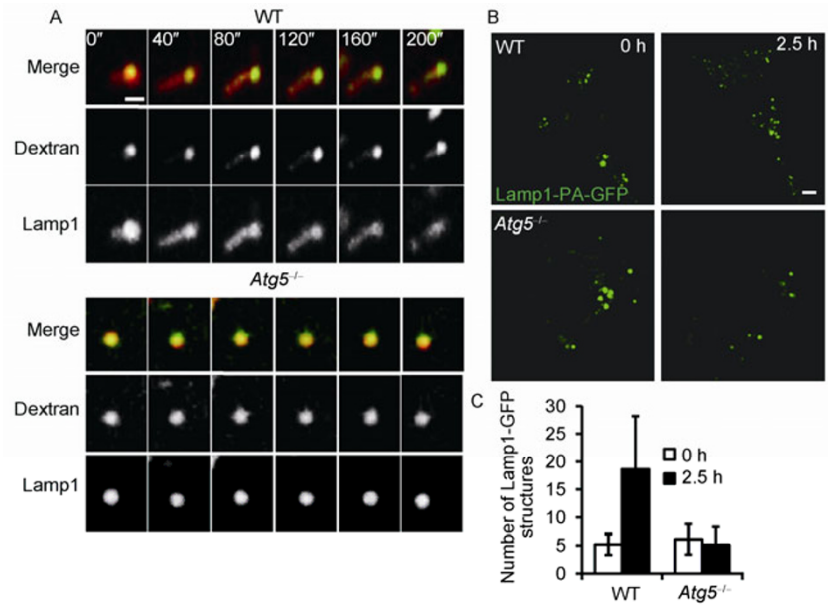

Figure 4 Tubulation and tubulation mediated fission of late endosomes from hybrid organelles are impaired in *Atg5*$^{-/-}$ MEF cell. A, Lamp1-cherry red-expressing wild type, *Atg5*$^{-/-}$ MEF cells were labeled with FITC-labeled dextran for 4 h; cells were washed and grown for another 20 h before imaging with spinning disc microscopy. Scale bar, 1 μm. B, Wild type, *Atg5*$^{-/-}$ MEF cells were transfected with Lamp1-photo-active GFP (Lamp1-PA-GFP); 18 h after transfection, Lamp1-PA-GFP was photo-activated by a 405 nm laser, and Lamp1-GFP-positive structures in the same cell were followed by time-lapse photography. Scale bar, 5 μm. C, Cells from (B) were quantified for the number of Lamp1-GFP structures. Fifty cells were counted. Error bars indicate the standard deviation.

mation subcomplex is a membrane bound heterodimer of sorting nexin (SNX) proteins [19]. SNX1, one of the SNX in retromer, transiently decorates endosome tubules during tabulation [20]. In wild type cells, SNX1 forms small puncta which can associate with LPOs. In *Atg5*$^{-/-}$ cells, the LPOs associated SNX1 puncta are markedly enlarged (Figure 5A and B), indicating SNX1 is accumulated in LPOs, implying retromer mediated retrieval of endosome components is likely impaired. To test this hypothesis, we monitored the retrieval of cation-independent mannose-6-phosphate receptor (CI-M6PR), a cargo of retromer by time lapse imaging. We found that the retrieval of CI-M6PR from hybrid organelles is indeed impaired in *Atg5*$^{-/-}$ cells (Figure 5C). Putting all these data together, we concluded that the defective late endosome and lysosome biogenesis is likely caused by impaired retromer-mediated retrieval of late endosome components from hybrid organelles.

2.6 Impaired V1-ATPase association on hybrid organelles in *Atg5*$^{-/-}$ cells

Since it is well established that the retrieval of M6PR from late endosomes is triggered by low pH within late endosomes, the blocking of M6PR retrieval indicates the possibility that the pH of endocytic organelles may be elevated in *Atg5*$^{-/-}$ cells. The pH of acidic vesicles is maintained by V-ATPase, which is composed of a membrane-anchored V0 domain and a detachable V1 domain [21,22]. The activity of V-ATPase is regulated by association and dissociation of the V1 domain from the V0 domain, the latter of which will result in elevated pH [21,22]. To test whether the recruitment of the V1 domain to acidic organelles is impaired in *Atg5*$^{-/-}$ cells, we loaded wild type and *Atg5*$^{-/-}$ cells with nano-gold particles for 4 h, resulting in accumulation of nano-gold particle in all organelles along the endocytic pathway. Since these labeled vesicles have a much higher density than other cell fractions, we were able to isolate endocytic vesicles with high purity. Using this technique, we found that the level of V-ATPase D is indeed markedly reduced on purified endocytic organelles in *Atg5*$^{-/-}$ cells (Figure 6A). Furthermore, knocking down the expression level of V-ATPase D recapitulated the abnormal numbers and morphology of LPOs in autophagy-defective cells (Figure 6B–D), indicating that V-ATPase D is necessary for maintenance of late endosome/lysosome biogenesis. Taken together, these data suggest that impaired recruitment of the V-ATPase V1 subunit to acidic organelles is likely the cause of defective late endosome/lysosome biogenesis.

2.7 Lowering intracellular pH restores late endosome/lysosome biogenesis

If the elevated pH is the cause of defective late endosome/lysosome biogenesis in *Atg5*$^{-/-}$ cells, we should be able to rescue the phenotype by lowering the pH in endocytic organelles. Maintaining cells in Ringer's buffer of different pHs can change the pH in endocytic organelles accordingly [23]. We found that by maintaining cells in slightly acidic

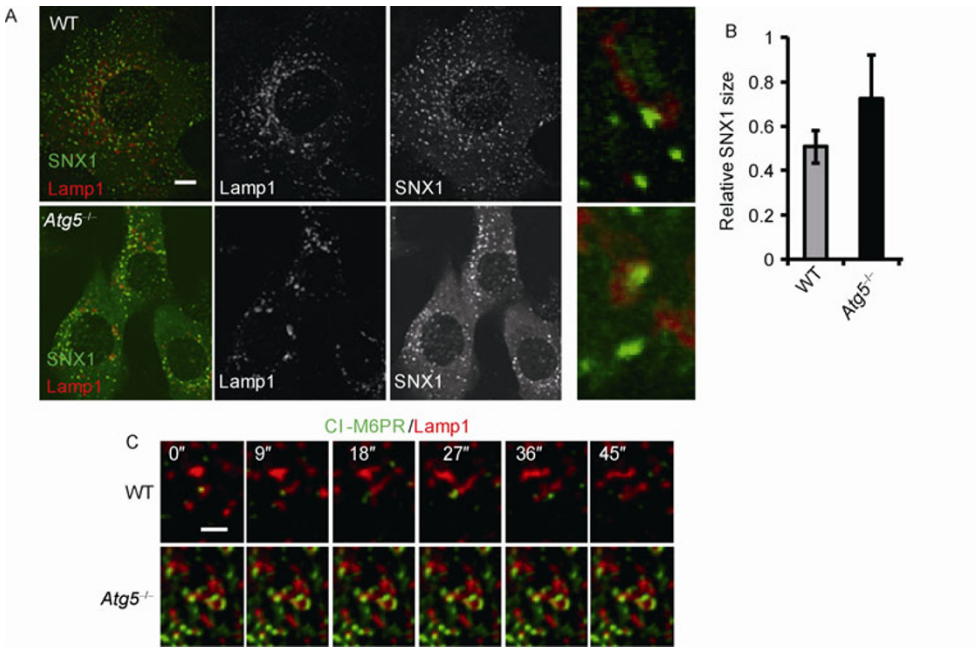

Figure 5 Impaired retrieval of late endosome components in autophagy null cells. A, Wild type, *Atg5*$^{-/-}$ MEF cells were transfected with SNX1-GFP and Lamp1-cherry red; 18 h after transfection, cells were observed by confocal microscopy. Scale bar, 5 um. B, Cells from (A) were quantified for the relative size of SNX1 size. Fifty cells were counted. Error bars indicate the standard deviation. C, Wild type, *Atg5*$^{-/-}$ MEF cells were transfected with CI-M6PR-GFP and Lamp1-cherry red; 18 h after transfection, hybrid organelles were followed by time-lapse photography using spinning disc microscopy. Scale bar, 1 μm.

Ringer's buffer for 20 min, the numbers and morphology of LPOs were almost completely restored to wild type levels (Figure 6E and F). Thus, we concluded that the elevation of pH is likely the cause of defective late endosome/lysosome biogenesis.

3 Discussion

In this manuscript, we have described a novel and unexpected function of Atg5 in maintaining late endosome/lysosome biogenesis. We showed that in *Atg5*$^{-/-}$ MEF cells, defective retrieval of late endosome components and fission of small Lamp1-positive vesicles from lysosome/late endosome hybrid organelles lead to defective formation of late endosomes and lysosomes (Figure 6G). At this point, we still do not fully understand the detailed molecular mechanism by which Atg5 regulates the formation of late endosome/lysosome. Our study suggested that the defective recruitment of V-ATPase D to acidic organelles, resulting in raised pH in these compartments, is likely responsible for defective late endosome/lysosome formation; however, at this point, we cannot rule out that Atg5 may affect late endosome/lysosome biogenesis through other mechanisms.

So far, there are two competing but not mutually exclusive models for lysosome biogenesis. In the "kiss and run" model, content mixing between late endosomes and lysosomes is through a series of transient, incomplete fusions. In the hybrid model, late endosomes fuse with pre-existing lysosomes to form hybrid organelles; the lysosome is presumably formed through a yet-to-be-identified retrieval process which eliminates late endosomal components [1,4]. Our study strongly supports the hybrid model, because we not only observed late endosome/lysosome hybrid organelles in wild type cells, but also showed that the biogenesis of late endosomes and lysosomes was arrested at the hybrid organelle stage in *Atg5*$^{-/-}$ cells. As a consequence, there were no mature late endosomes or lysosomes in these cells; thus, our study provides direct genetic evidence to support the hybrid model.

One interesting extension of the hybrid model revealed by our study is that the retrieval of Lamp1-positive vesicles from hybrid organelles is required for late endosome formation. The current model for late endosome formation suggests that late endosomes mature from early endosomes through selective removal of components unique to early endosomes and acquisition of late endosomal molecules. However, it is unclear how late endosomal components are acquired. Our study shows that the small Lamp1-positive vesicles derived from tubulation of hybrid organelles can fuse with early endosomes, thus likely contributing to late endosome formation by supplying retrieved late endosome components.

Does defective late endosome/lysosome biogenesis affect the degradation capacity of acidic organelles? We failed to detect a significant decrease in lysosomal protein degradation by DQ-BSA assay (data not shown). Similar observations have been reported in Chediak-Higashi syndrome

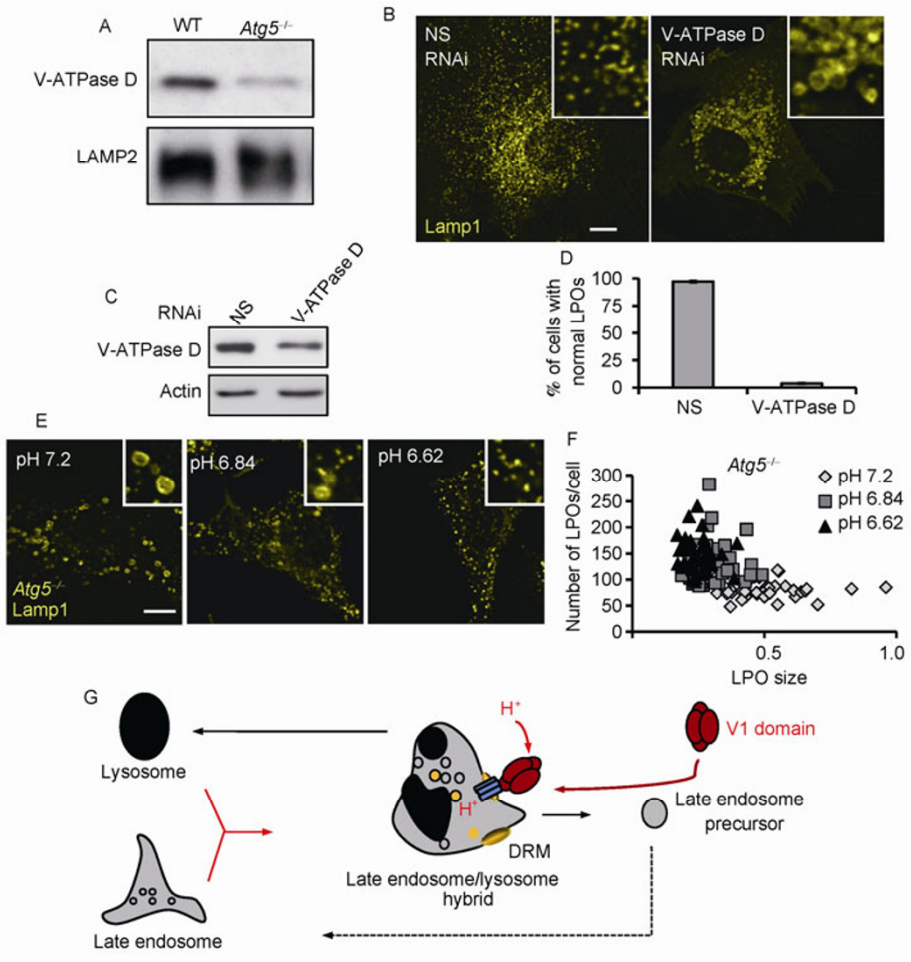

Figure 6 Impaired V-ATPase D recruitment to acidic organelles in *Atg5*$^{-/-}$ cell and lowering the intracellular pH rescue the abnormal LPO phenotype in *Atg5*$^{-/-}$ cells. A, Wild type, *Atg5*$^{-/-}$ MEF cells were loaded with nano-gold particles for 4 h; nano-gold particle-loaded organelles were isolated and analyzed for V-ATPase levels using Western blot. B, NRK cells were transfected with nonspecific (NS)- or V-ATPase D-RNAi. Cells were stained with antibody against Lamp1 and observed by confocal microscopy. Scale bar, 5 μm. C, Cells from (B) were analyzed for the expression level of V-ATPase by Western blot. D, Cells from (B) were assessed and quantified for normal LPOs in a blind fashion. One hundred cells were counted. Error bars indicate the standard deviation. E, *Atg5*$^{-/-}$ MEF cells were maintained in Ringer's buffer of different pH for 20 min; cells were stained with antibody against Lamp1 and observed by confocal microscopy. Scale bar, 5 μm. F, Cells from (E) were quantified for the number and size of Lamp1-positive compartments (LPO) in a blind fashion. Each symbol on the plot represents an individual cell. G, Model of Atg5 regulates lysosome and late endosome biogenesis.

(CHS) cells, which, like *Atg5*$^{-/-}$ cells, contain dramatically enlarged acidic organelles that cluster around nucleus; however, the overall lysosomal protein degradation capacity of CHS cells is not significantly altered [24].

If the degradation capacity of acidic organelles is not dramatically altered, does defective late endosome/lysosome biogenesis caused by Atg5 deficiency have any significant physiological relevance and pathological consequence? Again, Chediak-Higashi syndrome provides some clues. Chediak-Higashi syndrome is a severe disease which affects multiple body systems, especially the nervous and immune systems [25].

CHS is caused by mutations in the lysosomal trafficking regulator gene, *LYST*, and CHS cells display defective biogenesis of lysosome-related organelles [26]. The exact mechanism by which defective lysosome biogenesis has pathological consequences is still not fully understood; however, it is clear that defective lysosome biogenesis and trafficking is the underlying cause of these pathological features. The striking similarity between CHS and *Atg5*$^{-/-}$ cells implies that at least some of the pathological features observed in *Atg5*$^{-/-}$ models are likely caused by failure of late endosome and lysosome biogenesis.

We are grateful to N. Mizushima for providing Atg5$^{-/-}$ *MEF, Olympus China and the Tsinghua Cell Biology core facility for providing technical support, and to Dong Qi and Li Ying for assistance with confocal microscopy, TEM, and image processing. We thank Liu JiaJia for helpful discussions and J. Lippincott-Schwartz and J. Bonifacinofor for constructs and antibodies. This work was supported by the National Basic Research Program of China (2010CB833704 and 2011CB910100), the National Natural Science Foundation of China (31030043, 30971484, 31125018), and Tsinghua University (2010THZ0 and 2009THZ03071) to Yu Li.*

1 Luzio JP, Mullock BM, Pryor PR, Lindsay MR, James DE, Piper RC. Relationship between endosomes and lysosomes. Biochem Soc T, 2001, 29: 476–480
2 Luzio JP, Rous BA, Bright NA, Pryor PR, Mullock BM, Piper RC. Lysosome-endosome fusion and lysosome biogenesis. J Cell Sci, 2000, 113: 1515–1524
3 Gruenberg J, Stenmark H. The biogenesis of multivesicular endosomes. Nat Rev Mol Cell Biol, 2004, 5: 317–323
4 Luzio JP, Pryor PR, Bright NA. Lysosomes: fusion and function. Nat Rev Mol Cell Biol, 2007, 8: 622–632
5 Luzio JP, Rous BA, Bright NA, Pryor PR, Mullock BM, Piper RC. Lysosome-endosome fusion and lysosome biogenesis. J Cell Sci, 2000, 113(Pt 9): 1515–1524
6 Saftig P, Klumperman J. Lysosome biogenesis and lysosomal membrane proteins: trafficking meets function. Nat Rev Mol Cell Biol, 2009, 10: 623–635
7 Bright NA, Gratian MJ, Luzio JP. Endocytic delivery to lysosomes mediated by concurrent fusion and kissing events in living cells. Curr Biol: CB, 2005, 15: 360–365
8 Luzio JP, Pryor PR, Gray SR, Gratian MJ, Piper RC, Bright NA. Membrane traffic to and from lysosomes. Biochem Soc Symp, 2005, 77–86
9 Klionsky DJ, Emr SD. Autophagy as a regulated pathway of cellular degradation. Science, 2000, 290: 1717–1721
10 Mizushima N. Autophagy: process and function. Genes Dev, 2007, 21: 2861–2873
11 Xie Z, Klionsky DJ. Autophagosome formation: core machinery and adaptations. Nat Cell Biol, 2007, 9: 1102–1109
12 Tian Y, Li Z, Hu W, Ren H, Tian E, Zhao Y, Lu Q, Huang X, Yang P, Li X, Wang X, Kovács AL, Yu L, Zhang H. *C. elegans* screen identifies autophagy genes specific to multicellular organisms. Cell, 2010, 141: 1042–1055
13 Levine B, Mizushima N, Virgin HW. Autophagy in immunity and inflammation. Nature, 2011, 469: 323–335
14 Deretic V. Links between autophagy, innate immunity, inflammation and Crohn's disease. Dig Dis, 2009, 27: 246–251
15 Mizushima N, Noda T, Yoshimori T, Tanaka Y, Ishii T, George MD, Klionsky DJ, Ohsumi M, Ohsumi Y. A protein conjugation system essential for autophagy. Nature, 1998, 395: 395–398
16 Codogno P, Meijer AJ. Atg5: more than an autophagy factor. Nat Cell Biol, 2006, 8: 1045–1047
17 Hirst J, Futter CE, Hopkins CR. The kinetics of mannose 6-phosphate receptor trafficking in the endocytic pathway in HEp-2 cells: the receptor enters and rapidly leaves multivesicular endosomes without accumulating in a prelysosomal compartment. Mol Biol Cell, 1998, 9: 809–816
18 Wassmer T, Attar N, Harterink M, van Weering JR, Traer CJ, Oakley J, Goud B, Stephens DJ, Verkade P, Korswagen HC, Cullen PJ. The retromer coat complex coordinates endosomal sorting and dynein-mediated transport, with carrier recognition by the trans-Golgi network. Dev Cell, 2009, 17: 110–122
19 Cullen PJ, Korswagen HC. Sorting nexins provide diversity for retromer-dependent trafficking events. Nat Cell Biol, 2012, 14: 29–37
20 van Weering JR, Verkade P, Cullen PJ. SNX-BAR-mediated endosome tubulation is coordinated with endosome maturation. Traffic, 2012, 13: 94–107
21 Kane PM. Disassembly and reassembly of the yeast vacuolar H(+)-ATPase *in vivo*. J Biol Chem,1995, 270: 17025–17032
22 Kane PM, Parra KJ. Assembly and regulation of the yeast vacuolar H(+)-ATPase. J Exp Biol, 2000, 203: 81–87
23 Parton RG, Dotti CG, Bacallao R, Kurtz I, Simons K, Prydz K. pH-induced microtubule-dependent redistribution of late endosomes in neuronal and epithelial cells. J Cell Biol, 1991, 113: 261–274
24 Burkhardt JK, Wiebel FA, Hester S, Argon Y. The giant organelles in beige and Chediak-Higashi fibroblasts are derived from late endosomes and mature lysosomes. J Exp Med, 1993, 178: 1845–1856
25 Introne W, Boissy RE, Gahl WA. Clinical, molecular, and cell biological aspects of Chediak-Higashi syndrome. Mol Genet Metab, 1999, 68: 283–303
26 Barbosa MD, Nguyen QA, Tchernev VT, Ashley JA, Detter JC, Blaydes SM, Brandt SJ, Chotai D, Hodgman C, Solari RC, Lovett M, Kingsmore SF. Identification of the homologous beige and Chediak-Higashi syndrome genes. Nature, 1996, 382: 262–265

Supporting Information

Figure S1 Small LPOs derived from tabulation can fuse with early endosomes.

The supporting information is available online at life.scichina.com and link.springer.com. The supporting materials are published as submitted, without typesetting or editing. The responsibility for scientific accuracy and content remains entirely with the authors.